

Online-BLS: An Accurate and Efficient Online Broad Learning System for Data Stream Classification

Chunyu Lei¹, Guang-Ze Chen², C. L. Philip Chen¹ and Tong Zhang^{1,*}

¹South China University of Technology

²University of Macau

202210188289@mail.scut.edu.cn, chenguangze1999@gmail.com, philip.chen@ieee.org, tony@scut.edu.cn

Abstract

The state-of-the-art online learning models generally conduct a single online gradient descent when a new sample arrives and thus suffer from suboptimal model weights. To this end, we introduce an online broad learning system framework with closed-form solutions for each online update. Different from employing existing incremental broad learning algorithms for online learning tasks, which tend to incur degraded accuracy and expensive online update overhead, we design an effective weight estimation algorithm and an efficient online updating strategy to remedy the above two deficiencies, respectively. Specifically, an effective weight estimation algorithm is first developed by replacing notorious matrix inverse operations with Cholesky decomposition and forward-backward substitution to improve model accuracy. Second, we devise an efficient online updating strategy that dramatically reduces online update time. Theoretical analysis exhibits the splendid error bound and low time complexity of our model. The most popular test-then-training evaluation experiments on various real-world datasets prove its superiority and efficiency. Furthermore, our framework is naturally extended to data stream scenarios with concept drift and exceeds state-of-the-art baselines.

1 Introduction

Online Learning (OL) [Hoi *et al.*, 2021] provides a crucial solution for learning knowledge from various real-world data streams, such as weather [Elwell and Polikar, 2011], call record [Swithinbank *et al.*, 1977], and stock market trading data [Hu *et al.*, 2015]. Typical OL algorithms involve learning model weights from one by one instance [Gunasekara *et al.*, 2023]. The generic OL pipeline is as follows: 1) The initial model comes with zero or random weights because no samples are received. 2) When a new sample arrives, its model weights are rapidly updated to provide a more accurate prediction for subsequent arrivals [Yuan *et al.*, 2022]. Thus, a brilliant OL model must be efficient and accurate.

While appealing, existing state-of-the-art OL models are generally optimized based on gradient descent algorithms [Wen *et al.*, 2024; Su *et al.*, 2024]. To be specific, when a new sample arrives, all of them execute an error backpropagation and weight update process. Thus, none of them can achieve an optimal solution for model weights.

Recently, Broad Learning System (BLS) has been proposed as an efficient batch or incremental machine learning model [Chen and Liu, 2018; Chen *et al.*, 2019; Gong *et al.*, 2022]. First, BLS utilizes sparse coding to map raw data to a low-dimensional feature space to form feature nodes. The enhancement nodes are then obtained by random orthogonal transformation and non-linear mapping of the feature nodes. Finally, feature and enhancement nodes are cascaded, and then the relation weights between them and ground truth are estimated by the ridge regression algorithm. Thus, its closed-form solutions and incremental learning capabilities shed light on tackling the above OL issue.

To address the suboptimal model weight issue, it is urgent to develop a novel OL framework based on BLS with closed-form solutions. Fortunately, various data incremental BLS algorithms [Chen and Liu, 2018; Fu *et al.*, 2022; Du *et al.*, 2024; Zhong *et al.*, 2024] have been proposed to enhance accuracy and robustness. By setting the number of training samples for each increment to 1, most of them can inherently tackle online machine learning tasks. Thanks to the outstanding generalization of BLS, most of them can also rigorously guarantee the optimality for each online model update. Despite the straightforwardness, they still face challenges in online machine learning tasks. The common and most urgent issue is that all of them are based on the matrix inverse operation, still with high computational complexity and low numerical stability. It means that many errors are incurred when solving for online model weights. In other words, their accuracy and efficiency need to be improved.

In this paper, we develop a native Online-BLS framework to address the suboptimality issue of OL model weights. To our knowledge, this paper clarifies the above issue for the first time and succeeds in solving it using our Online-BLS framework. Its technical innovations are summarized as follows. First, we deduce an Effective Weight Estimation Algorithm (EWEA) based on Cholesky factorization and forward-backward substitution, which significantly improves the accuracy of Online-BLS and offers excellent the-

*Corresponding Author

oretical error bounds. Second, an Efficient Online Updating Strategy (EOUS) is designed based on the rank-one update algorithm of the Cholesky factor [Gill *et al.*, 1974; SEGER, 2007] to improve the efficiency of Online-BLS. The time complexity analysis shows a significant reduction in time overhead. Furthermore, to demonstrate the superiority and flexibility of our Online-BLS framework, we propose a straightforward extension to achieve non-stationary data stream classification. Finally, the superiority and efficiency of Online-BLS are empirically confirmed by a comprehensive comparison with baselines.

2 Related Work

2.1 Online Learning

OL is a family of machine learning algorithms for learning models incrementally from sequential data [Hoi *et al.*, 2021]. Existing OL algorithms fall into two main categories. The first category refers to traditional OL algorithms modified from traditional machine learning models. Hoeffding Tree (HT) has been proposed to construct a decision tree online from data streams [Hulten *et al.*, 2001]. Subsequently, an Adaptive Random Forest (ARF) has been developed to handle concept drift scenarios [Gomes *et al.*, 2017]. Specifically, once concept drift is detected, ARF resets its base tree to adapt to the new concept. Moreover, traditional online machine learning methods also include Passive Aggressive (PA) [Crammer *et al.*, 2006], Perceptron [Rosenblatt, 1958], Leveraging Bagging (LB) [Bifet *et al.*, 2010], etc. Despite simplicity, all of them fail to extract effective features from streaming data and thus degrade their accuracy.

Inspired by deep learning [Larochelle *et al.*, 2009; Zhang *et al.*, 2021], the second one is online deep learning, which aims to learn a deep neural network online. To be specific, Online Gradient Descent (OGD) has been proposed to update its weights with gradient when a sample arrives [Zinkevich, 2003]. Given that network depth is difficult to determine in advance, [Sahoo *et al.*, 2018] proposed the Hedge Backpropagation (HBP) to dynamically integrate multiple layers of neural networks, which is of great significance for subsequent research. Subsequently, [Ashfahani and Pratama, 2019] proposed Autonomous Deep Learning (ADL) that can construct its network structure from scratch by adjusting its depth and width without an initial one. To solve the online hyperparameter optimization challenge of neural networks, Continuously Adaptive Neural network for Data streams (CAND) [Gunnasekara *et al.*, 2022] has been proposed, which chooses the best model from a candidate pool of neural networks trained with different hyperparameters combination. Adaptive Tree-like Neural Network (ATNN) has been proposed to solve the catastrophic forgetting problem by choosing suitable positions on the backbone to grow branches for the new concept [Wen *et al.*, 2024]. To address concept drift and sub-network optimization conflict issues, EODL has been proposed, including depth adaption and parameter adaption strategies [Su *et al.*, 2024]. Despite significant progress, none of them avoids gradient descent. They execute an error backpropagation and weight update when a sample arrives. However, these algorithms are far from enough to ensure the

optimality of their model weights in the subsequent sample prediction. Hence, developing an OL framework based on closed-form solutions becomes crucial.

2.2 Incremental Broad Learning System

Due to its efficiency and versatility, BLS has been widely used for a variety of tasks [Lei *et al.*, 2024; Gong *et al.*, 2024; Guo *et al.*, 2024; Yun *et al.*, 2024; Zhang *et al.*, 2024]. In particular, substantial works have been presented for incremental machine learning tasks. The first data incremental algorithm for BLS is deduced from Greville’s theory [Greville, 1960], which we refer to I-BLS in this paper [Chen and Liu, 2018]. However, the performance of I-BLS dramatically degrades when learning a new class or task. To this end, TiBLS and BLS-CIL have been proposed based on residual learning and graph regularization, respectively [Fu *et al.*, 2022; Du *et al.*, 2024]. Furthermore, motivated by the fact that I-BLS still fails to improve accuracy when the size of the training data is not roughly equal for each addition, Zhong *et al.* have proposed a Robust Incremental BLS (RI-BLS) [Zhong *et al.*, 2024]. Among them, TiBLS stacks a new BLS module on the current model whenever a new task arrives. It views each new training sample as a new task in an online machine learning scenario. Therefore, a new BLS model needs to be learned. Inevitably, it imposes an expensive computational overhead and does not meet the requirements for efficient OL. In contrast, the remaining three algorithms only need to fine-tune their weights based on new arrivals, which is relatively efficient. The details of these incremental BLS algorithms are presented in Appendix A. Despite their feasibility, none of them can avoid matrix inversion operations. Thus, the defects of matrix inversion come along with them.

3 Method

3.1 Problem Setting

This paper focuses on online classification tasks. The input data sequence can be represented as $\mathbf{X} = \{(\mathbf{x}_k, \mathbf{y}_k) | k = 1, 2, \dots, n\}$, where $\mathbf{x}_k \in \mathbb{R}^d$ denotes the k -th sample with d feature values and $\mathbf{y}_k \in \mathbb{R}^c$ is the one-hot target corresponding to \mathbf{x}_k . c is the total number of categories. When a sample \mathbf{x}_k arrives, the prediction $\hat{\mathbf{y}}_k$ is derived first. Subsequently, the online learning model makes an update using the real label \mathbf{y}_k .

3.2 Online-BLS Framework

In this section, we derive an Online-BLS framework. It provides a closed-form solution for each online update step and therefore resolves the issue of suboptimal online model weights.

Given the first sample $\mathbf{x}_1 \in \mathbb{R}^d$, the i -th feature node group $\mathbf{z}_i \in \mathbb{R}^{n_1}$ and j -th enhancement node group $\mathbf{h}_j \in \mathbb{R}^{n_3}$ are defined as

$$\mathbf{z}_i^\top = \phi(\mathbf{x}_1^\top \mathbf{W}_{f_i} + \beta_{f_i}^\top), i = 1, 2, \dots, n_2, \quad (1)$$

$$\mathbf{h}_j^\top = \sigma(\mathbf{x}_1^\top \mathbf{W}_{e_j} + \beta_{e_j}^\top), j = 1, 2, \dots, n_4. \quad (2)$$

Here, $\mathbf{W}_{f_i} \in \mathbb{R}^{d \times n_1}$, $\mathbf{W}_{e_j} \in \mathbb{R}^{n_1 n_2 \times n_3}$, $\beta_{f_i} \in \mathbb{R}^{n_1}$, and $\beta_{e_j} \in \mathbb{R}^{n_3}$ are randomly generated. $\phi(\cdot)$ and $\sigma(\cdot)$ are gener-

ally a linear transformation and a nonlinear activation, respectively. Through incorporating linear and non-linear features, the broad features \mathbf{a}_1 can be expressed as

$$\mathbf{a}_1^\top \triangleq [\mathbf{z}_1^\top, \dots, \mathbf{z}_{n_2}^\top, \mathbf{h}_1^\top, \dots, \mathbf{h}_{n_4}^\top] \quad (3)$$

Then, the prediction of \mathbf{x}_1 can be calculated as $\hat{\mathbf{y}}_1^\top = \mathbf{a}_1^\top \mathbf{W}^{(0)}$, where $\mathbf{W}^{(0)}$ is a zero matrix. After \mathbf{y}_1 is revealed, our optimization problem is expressed as

$$\mathbf{W}^{(1)} = \arg \min_{\mathbf{W}} \|\mathbf{a}_1^\top \mathbf{W} - \mathbf{y}_1^\top\|^2 + \lambda \|\mathbf{W}\|^2, \quad (4)$$

where $|\cdot|$ denotes the L_2 norm. Since equation 4 is a convex optimization problem, we derive its gradient with respect to \mathbf{W} and set it to 0. Then, we have

$$(\mathbf{a}_1 \mathbf{a}_1^\top + \lambda \mathbf{I}) \mathbf{W} = \mathbf{a}_1 \mathbf{y}_1^\top. \quad (5)$$

When the k -th sample \mathbf{x}_k ($k = 2, 3, \dots, n$) arrives, \mathbf{a}_k is obtained by replacing \mathbf{x}_1 in equations 1 and 2 with \mathbf{x}_k . Then, its prediction is $\hat{\mathbf{y}}_k^\top = \mathbf{a}_k^\top \mathbf{W}^{(k-1)}$. Suppose we retrain $\mathbf{W}^{(k)}$ with the first k samples, equation 5 becomes

$$([\mathbf{a}_1, \dots, \mathbf{a}_k] \begin{bmatrix} \mathbf{a}_1^\top \\ \vdots \\ \mathbf{a}_k^\top \end{bmatrix} + \lambda \mathbf{I}) \mathbf{W} = [\mathbf{a}_1, \dots, \mathbf{a}_k] \begin{bmatrix} \mathbf{y}_1^\top \\ \vdots \\ \mathbf{y}_k^\top \end{bmatrix}. \quad (6)$$

Let $\mathbf{K}^{(1)} = \mathbf{a}_1 \mathbf{a}_1^\top + \lambda \mathbf{I}$, we have

$$\begin{aligned} \mathbf{K}^{(k)} &= [\mathbf{a}_1, \dots, \mathbf{a}_k] \begin{bmatrix} \mathbf{a}_1^\top \\ \vdots \\ \mathbf{a}_k^\top \end{bmatrix} + \lambda \mathbf{I} \\ &= \mathbf{K}^{(k-1)} + \mathbf{a}_k \mathbf{a}_k^\top, \end{aligned} \quad (7)$$

and

$$\begin{aligned} [\mathbf{a}_1, \dots, \mathbf{a}_k] \begin{bmatrix} \mathbf{y}_1^\top \\ \vdots \\ \mathbf{y}_k^\top \end{bmatrix} &= \sum_{i=1}^{k-1} \mathbf{a}_i \mathbf{y}_i^\top + \mathbf{a}_k \mathbf{y}_k^\top \\ &= \mathbf{K}^{(k-1)} \mathbf{W}^{(k-1)} + \mathbf{a}_k \mathbf{y}_k^\top \\ &= (\mathbf{K}^{(k)} - \mathbf{a}_k \mathbf{a}_k^\top) \mathbf{W}^{(k-1)} + \mathbf{a}_k \mathbf{y}_k^\top \\ &= \mathbf{K}^{(k)} \mathbf{W}^{(k-1)} - \mathbf{a}_k (\mathbf{a}_k^\top \mathbf{W}^{(k-1)} - \mathbf{y}_k^\top). \end{aligned} \quad (8)$$

Substituting equation 8 into 6, we have

$$\mathbf{K}^{(k)} \Delta \mathbf{W} = \mathbf{B}^{(k)}, \quad (9)$$

where $\Delta \mathbf{W} = \mathbf{W} - \mathbf{W}^{(k-1)}$ and $\mathbf{B}^{(k)} = \mathbf{a}_k (\mathbf{y}_k^\top - \mathbf{a}_k^\top \mathbf{W}^{(k-1)})$.

Importantly, the right-hand terms of equations 5 and 9 are equal when k is equal to 1 (i.e., $\mathbf{B}^{(1)} = \mathbf{a}_1 \mathbf{y}_1^\top$). Thus, we conclude that the matrix $\mathbf{W}^{(1)}$ solved via equations 5 and 9 is equivalent if and only if $\mathbf{W}^{(0)} = \mathbf{0}$ and $\mathbf{K}^{(0)} = \lambda \mathbf{I}$. In other words, we only need to solve equation 9 to get $\Delta \mathbf{W}^{(k)}$. Then, we have

$$\mathbf{W}^{(k)} = \mathbf{W}^{(k-1)} + \Delta \mathbf{W}^{(k)}, \quad k = 1, 2, \dots, n. \quad (10)$$

Since equation 9 has a closed-form solution, our Online-BLS framework is completed without a gradient descent step. The algorithms for accurately and efficiently deriving closed-form solutions to equation 9 will be described in later sections.

3.3 Effective Weight Estimation Algorithm

To solve $\Delta \mathbf{W}$ accurately, we propose an efficient weight estimation algorithm based on Cholesky factorization and forward-backward substitution. After the Cholesky factorization of $\mathbf{K}^{(k)}$ to obtain the Cholesky factor $\mathbf{L}^{(k)}$, equation 9 can be solved via the following two equations:

$$\mathbf{L}^{(k)} \mathbf{C} = \mathbf{B}^{(k)}, \quad (11)$$

$$(\mathbf{L}^{(k)})^\top \Delta \mathbf{W} = \mathbf{C}. \quad (12)$$

Denotes $\mathbf{B}^{(k)} = [\mathbf{b}_1, \dots, \mathbf{b}_m]^\top$, using the forward and backward substitution, the solutions of equations 11 and 12 are

$$\mathbf{c}_i^\top = (\mathbf{b}_i^\top - \sum_{d=1}^{i-1} l_{di}^{(k)} \mathbf{c}_d^\top) / l_{ii}^{(k)}, \quad i = 1, \dots, m \quad (13)$$

and

$$(\Delta \mathbf{w}_i^{(k)})^\top = \left(\mathbf{c}_i^\top - \sum_{d=i+1}^m l_{id}^{(k)} (\Delta \mathbf{w}_d^{(k)})^\top \right) / l_{ii}^{(k)}, \quad i = m, \dots, 1, \quad (14)$$

respectively. Then, our weight matrix $\mathbf{W}^{(k)}$ can be obtained online by equation 10 without the numerically unstable matrix inverse operation. The error bounds are discussed in Section 4.1.

3.4 Efficient Online Update Strategy

To avoid expensive Cholesky decompositions for each online update, we discuss below how to efficiently derive $\mathbf{L}^{(k)}$ from $\mathbf{L}^{(k-1)}$ and \mathbf{a}_k . Inspired by the rank-one update strategy [SEEEGER, 2007], we first cascade the k -th broad feature \mathbf{a}_k and the previous Cholesky factor $\mathbf{L}^{(k-1)}$ as $[\mathbf{a}_k, \mathbf{L}^{(k-1)}]$. Undergoing a series of orthogonal Givens rotations, we have

$$\mathbf{G} \begin{bmatrix} \mathbf{a}_k^\top \\ (\mathbf{L}^{(k-1)})^\top \end{bmatrix} = \begin{bmatrix} \mathbf{0}^\top \\ \bar{\mathbf{L}}^\top \end{bmatrix}, \quad (15)$$

where \mathbf{G} is a sequence of Givens matrices of the form $\mathbf{G} = \mathbf{G}_m \mathbf{G}_{m-1} \dots \mathbf{G}_1$. Then, we have

$$\begin{aligned} [\mathbf{0}, \bar{\mathbf{L}}] \begin{bmatrix} \mathbf{0}^\top \\ \bar{\mathbf{L}}^\top \end{bmatrix} &= \bar{\mathbf{L}} \bar{\mathbf{L}}^\top \\ &= [\mathbf{a}_k, \mathbf{L}^{(k-1)}] \underbrace{\mathbf{G}^\top \mathbf{G}}_{=\mathbf{I}} \begin{bmatrix} \mathbf{a}_k^\top \\ (\mathbf{L}^{(k-1)})^\top \end{bmatrix} \\ &= \mathbf{L}^{(k-1)} (\mathbf{L}^{(k-1)})^\top + \mathbf{a}_k \mathbf{a}_k^\top \end{aligned} \quad (16)$$

Thus, $\bar{\mathbf{L}} = \mathbf{L}^{(k)}$ is the updated Cholesky factor we need. To rotate $a_{ki} = 0$, we construct the Givens matrix as follows:

$$\mathbf{G}_i = \mathbf{I} + (c_i - 1)(\mathbf{e}_1 \mathbf{e}_1^\top + \mathbf{e}_i \mathbf{e}_i^\top) + s_i(\mathbf{e}_i \mathbf{e}_1^\top - \mathbf{e}_1 \mathbf{e}_i^\top),$$

where $c_i = l_{ii}^{(k)} / \sqrt{(l_{ii}^{(k)})^2 + a_{ki}^2}$, $s_i = a_{ki} / \sqrt{(l_{ii}^{(k)})^2 + a_{ki}^2}$, and \mathbf{e}_i denotes a standard unit vector with $e_{ii} = 1$.

Remark 1. The Cholesky factor requires that the elements on the main diagonal are greater than 0. Thus, if $\bar{\mathbf{L}}_{ii} < 0$, we simply flip $c_i \leftarrow -c_i$ and $s_i \leftarrow -s_i$. Then, $\bar{\mathbf{L}}_{ii} > 0$ becomes satisfied.

Algorithm 1 Online-BLS Algorithm

Input: Stream data $\mathbf{X} = \{(\mathbf{x}_k, \mathbf{y}_k) | k = 1, 2, \dots, n\}$, parameters n_1, n_2, n_3, n_4 , and λ .
Output: Prediction results $\hat{\mathbf{y}}_1, \dots, \hat{\mathbf{y}}_n$.

- 1: Initial $\mathbf{W}^{(0)} = \mathbf{0}$, $\mathbf{L}^{(0)} = \text{Chol}(\lambda \mathbf{I})$
- 2: **for** $k = 1, 2, \dots, n$ **do**
- 3: Receive instance: \mathbf{x}_k
- 4: Obtain broad feature \mathbf{a}_k via equations 1, 2, and 3
- 5: Predict $\hat{\mathbf{y}}_k^\top = \mathbf{a}_k^\top \mathbf{W}^{(k-1)}$ and then reveal \mathbf{y}_k
- 6: Obtain the updated factor $\mathbf{L}^{(k)}$ by equation 15
- 7: Obtain $\mathbf{W}^{(k)}$ by equations 13, 14, and 10.
- 8: **end for**

Algorithm 2 Handling Concept Drift

Input: Stream data $\mathbf{X} = \{(\mathbf{x}_k, \mathbf{y}_k) | k = 1, 2, \dots, n\}$, parameters $n_1, n_2, n_3, n_4, \lambda$, and decay factor μ .
Output: Prediction results $\hat{\mathbf{y}}_1, \dots, \hat{\mathbf{y}}_n$.

- 1: Initial $\mathbf{W}^{(0)} = \mathbf{0}$, $\mathbf{P}^{(0)} = \mathbf{0}$
- 2: **for** $k = 1, 2, \dots, n$ **do**
- 3: Receive instance: \mathbf{x}_k
- 4: Obtain broad feature \mathbf{a}_k via equations 1, 2, and 3
- 5: Predict $\hat{\mathbf{y}}_k^\top = \mathbf{a}_k^\top \mathbf{W}^{(k-1)}$ and then reveal \mathbf{y}_k
- 6: $\mathbf{P}^{(k)} = \mu \mathbf{P}^{(k-1)} + \mathbf{a}_k \mathbf{a}_k^\top$, $\mathbf{L}^{(k)} = \text{Chol}(\mathbf{P}^{(k)} + \lambda \mathbf{I})$
- 7: Obtain $\mathbf{W}^{(k)}$ by equations 13, 14, and 10.
- 8: **end for**

Remark 2. The function $\text{Chol}(\mathbf{M})$ refers to the Cholesky factorization of \mathbf{M} and returns its lower triangular factor \mathbf{L} .

The Online-BLS algorithm is summarized in Algorithm 1.

3.5 Handling Concept Drift

Concept drift is a common challenge in data streams, where the joint distribution of features and labels changes over time. Existing BLS algorithms cannot handle concept drift scenarios in online learning. Thanks to the flexibility of our Online-BLS framework, we are able to adopt a simple solution to the concept drift problem, by modifying two lines of code upon Algorithm 1, which is listed in Algorithm 2. The core idea is that learning the time-varying concept with new data is better than with old one. Technically, more attention to new data is encouraged by multiplying history by a decay factor μ .

4 Theoretical Analysis

4.1 Error Bound

The following lemmas are first introduced before deriving theoretical errors.

Lemma 1. The solution $\hat{\mathbf{W}}$ derived via forward substitution satisfies

$$(\mathbf{L} + \boldsymbol{\Gamma}_1) \hat{\mathbf{W}} = \mathbf{Y}, \quad |\boldsymbol{\Gamma}_1| \leq C_m u |\mathbf{L}| + \mathcal{O}(u^2), \quad (17)$$

where $\mathbf{L} \in \mathbb{R}^{m \times m}$ is a lower triangular matrix, C_m denotes a constant positively correlated with m , and $\mathcal{O}(u^2)$ represents the error tail term.

The detailed proof can be referred to [Higham, 2002]. Lemma 1 states that its solution satisfies a slightly perturbed system. Also, each entry in the perturbation matrix $\boldsymbol{\Gamma}_1$ is much smaller than the corresponding element in \mathbf{L} .

Remark 3 (Definition of u). $\forall x \in \mathbb{R}$, its floating-point representation is given by $fl(x) = x(1 + \gamma)$, where γ is the floating-point error and its upper bound, unit roundoff u , (i.e., $|\gamma| \leq u$) can be defined as

$$u = \frac{1}{2} \times (\text{gap between 1 and next largest floating point number}).$$

To be specific, the unit roundoff for IEEE single format is about 10^{-7} and for double format is about 10^{-16} .

Lemma 2. The solution $\hat{\mathbf{W}}$ derived via backward substitution satisfies

$$(\mathbf{L}^\top + \boldsymbol{\Gamma}_2) \hat{\mathbf{W}} = \mathbf{Y}, \quad |\boldsymbol{\Gamma}_2| \leq C_m u |\mathbf{L}^\top| + \mathcal{O}(u^2), \quad (18)$$

where \mathbf{L}^\top is an upper triangular matrix.

The proof also refers to [Higham, 2002].

Error Bound of Online-BLS. Recall that the incremental weight $\Delta \mathbf{W}^{(k)}$ in Online-BLS is solved via equations 11 and 12. Therefore, the error bound is given in Theorem 1. For brevity, we omit the superscript (k) in the following.

Theorem 1. Let $\hat{\mathbf{L}}$ be the estimated Cholesky factor \mathbf{L} , we have

$$\hat{\mathbf{L}} \hat{\mathbf{L}}^\top \Delta \hat{\mathbf{W}} = (\mathbf{L} \mathbf{L}^\top + \boldsymbol{\Gamma}) \Delta \hat{\mathbf{W}} = \mathbf{B}$$

with

$$\begin{aligned} |\mathbf{B} - \mathbf{L} \mathbf{L}^\top \Delta \hat{\mathbf{W}}| &= |\boldsymbol{\Gamma}| |\Delta \hat{\mathbf{W}}| \\ &\leq C_m u |\mathbf{L}| |\mathbf{L}^\top| |\Delta \hat{\mathbf{W}}| + \mathcal{O}(u^2). \end{aligned} \quad (19)$$

Proof. From Lemmas 1 and 2, we have

$$\begin{aligned} (\mathbf{L} + \boldsymbol{\Gamma}_1) \hat{\mathbf{C}} &= \mathbf{B}, \quad |\boldsymbol{\Gamma}_1| \leq C_m u |\mathbf{L}| + \mathcal{O}(u^2), \\ (\mathbf{L}^\top + \boldsymbol{\Gamma}_2) \Delta \hat{\mathbf{W}} &= \hat{\mathbf{C}}, \quad |\boldsymbol{\Gamma}_2| \leq C_m u |\mathbf{L}^\top| + \mathcal{O}(u^2), \end{aligned}$$

and thus

$$\begin{aligned} \mathbf{B} &= (\mathbf{L} + \boldsymbol{\Gamma}_1)(\mathbf{L}^\top + \boldsymbol{\Gamma}_2) \Delta \hat{\mathbf{W}} \\ &= (\mathbf{L} \mathbf{L}^\top + \mathbf{L} \boldsymbol{\Gamma}_2 + \boldsymbol{\Gamma}_1 \mathbf{L}^\top + \boldsymbol{\Gamma}_1 \boldsymbol{\Gamma}_2) \Delta \hat{\mathbf{W}}. \end{aligned}$$

Thus, we find $(\mathbf{L} \mathbf{L}^\top + \boldsymbol{\Gamma}) \Delta \hat{\mathbf{W}} = \mathbf{B}$ with

$$|\mathbf{B}| \leq |\mathbf{L}| |\boldsymbol{\Gamma}_2| + |\boldsymbol{\Gamma}_1| |\mathbf{L}^\top| + \mathcal{O}(u^2) \leq C_m u |\mathbf{L}| |\mathbf{L}^\top| + \mathcal{O}(u^2),$$

such that

$$\begin{aligned} |\mathbf{B} - \mathbf{L} \mathbf{L}^\top \Delta \hat{\mathbf{W}}| &= |\boldsymbol{\Gamma}| |\Delta \hat{\mathbf{W}}| \\ &\leq C_m u |\mathbf{L}| |\mathbf{L}^\top| |\Delta \hat{\mathbf{W}}| + \mathcal{O}(u^2). \end{aligned}$$

Thus, we can conclude equation 19. \square

Error Bound of Inverse Methods. As for the previous I-BLS, BLS-CIL, and RI-BLS, none of them avoids computing the inverse of a large matrix, which means to obtain $\Delta \mathbf{W} = fl((\mathbf{A}^\top \mathbf{A} + \lambda \mathbf{I})^{-1} \mathbf{B})$ only with rounding errors. Then, we have

$$\begin{aligned} \Delta \hat{\mathbf{W}} &= ((\mathbf{A}^\top \mathbf{A} + \lambda \mathbf{I})^{-1} + \boldsymbol{\Gamma}) \mathbf{B}, \\ |\boldsymbol{\Gamma}| &\leq C_m u |(\mathbf{A}^\top \mathbf{A} + \lambda \mathbf{I})^{-1}| + \mathcal{O}(u^2) \end{aligned}$$

Method	Time Complexity
I-BLS	$\mathcal{O}(km + m^2 + m^3 + mc)/\mathcal{O}(km + m + mc)$
BLS-CIL	$\mathcal{O}(m^3 + m^2c + m^2 + mc + m)$
RI-BLS	$\mathcal{O}(m^3 + m^2c + m^2 + mc)$
Ours	$\mathcal{O}(m^2c + m^2 + mc)$

Table 1: Time complexity

and $(\mathbf{A}^\top \mathbf{A} + \lambda \mathbf{I})\Delta \hat{\mathbf{W}} = \mathbf{B} + (\mathbf{A}^\top \mathbf{A} + \lambda \mathbf{I})\mathbf{F}\mathbf{B}$. Thus, its error bound is

$$\begin{aligned} & |\mathbf{B} - (\mathbf{A}^\top \mathbf{A} + \lambda \mathbf{I})\Delta \hat{\mathbf{W}}| \\ & \leq C_m u |(\mathbf{A}^\top \mathbf{A} + \lambda \mathbf{I})| |(\mathbf{A}^\top \mathbf{A} + \lambda \mathbf{I})^{-1}| |\mathbf{B}| + \mathcal{O}(u^2) \\ & \leq C_m u |\mathbf{L}| |\mathbf{L}^\top| |(\mathbf{A}^\top \mathbf{A} + \lambda \mathbf{I})^{-1}| |\mathbf{B}| + \mathcal{O}(u^2) \quad (20) \end{aligned}$$

Observing equations 19 and 20, since \mathbf{A} is generally an ill-conditioned matrix for BLS, there exists $|\Delta \hat{\mathbf{W}}| \ll |(\mathbf{A}^\top \mathbf{A} + \lambda \mathbf{I})^{-1}| |\mathbf{B}|$. Thus, matrix inverse methods provide higher error bounds than ours.

4.2 Time Complexity

The time complexities of our Online-BLS and three existing incremental BLS are shown in Table 1. First, the time complexity of I-BLS contains the primary term of k . That is, as the number of samples received by I-BLS increases, its online update time overhead increases linearly. This is quite terrible for online learning tasks, which tend to have a lot or even an infinite number of samples. By comparing the time complexity of ours and the remaining two methods, we find that RI-BLS and BLS-CIL have one (i.e., m^3) and two (i.e., m^3 and m) additional terms over Online-BLS, respectively. Thus, our Online-BLS algorithm is remarkably efficient and well suitable for online machine learning tasks.

5 Experiments

The most common prequential test-then-train experimental paradigm is adopted. First, Online-BLS is compared with state-of-the-art incremental BLS algorithms on the six real-world stationary datasets. Then, parameter sensitivity analysis experiments are performed to verify the stability of Online-BLS. Third, ablation experiments are performed by removing EOUS from our method. Finally, additional experiments are performed on the four non-stationary datasets to demonstrate the superiority of our approach over state-of-the-art baselines. Table 2 and Appendix B summarize and detail the dataset used. The metrics used in this paper are detailed in Appendix C. All experiments are conducted on the Ubuntu 20.04 operating system, and the CPU is AMD EPYC 7302.

5.1 Experiments on Stationary Datasets

The comparison methods include I-BLS [Chen and Liu, 2018], BLS-CIL [Du *et al.*, 2024], and RI-BLS [Zhong *et al.*, 2024]. To ensure fairness, we set the parameters common to all comparison methods and Online-BLS to be the same. Specifically, n_1 , n_2 , n_3 , and n_4 were set to 10, 10, 1000, and 1, respectively. The regularization parameter λ was set to

Dataset	IA	C	DP	Type
IS	19	7	2,310	Stationary
USPS	256	10	9,298	Stationary
Letter	16	26	20,000	Stationary
Adult	14	2	45,222	Stationary
Shuttle	8	7	58,000	Stationary
MNIST	784	10	70,000	Stationary
Hyperplane	20	2	100,000	Concept Drift
SEA	3	2	100,000	Concept Drift
Electricity	6	2	45,312	Concept Drift
CoverType	54	7	581,012	Concept Drift

Table 2: Descriptions of datasets. IS: Image Segment; IA: Input Attributes; C: Classes; DP: Data Points.

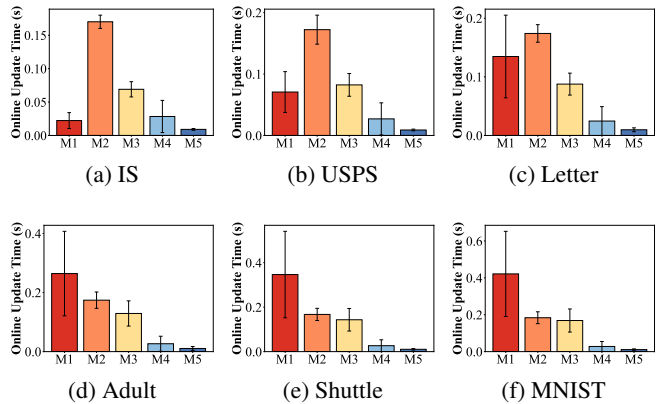


Figure 1: Average and Standard Deviation (SD) of online update time. M1: I-BLS; M2: BLS-CIL; M3: RI-BLS; M4: Ours w/o EOUS; M5: Ours.

$1e-8$ for I-BLS, RI-BLS and Online-BLS. For BLS-CIL, λ_1 and λ_2 were set to 1 in the original paper, which is unstable in the online learning task. Therefore, we tuned both to 0.1 to obtain better performance. To draw credible conclusions, we repeated each experiment 10 times by changing the order of streaming data and the initialization parameters.

The average and Standard Deviation (SD) of the final Online Cumulative Accuracies (OCA) for all methods are shown in Table 3. First, our proposed Online-BLS exceeds all the baselines on 5 out of 6 datasets. For the USPS dataset, the OCA of Online-BLS is also very close to the highest one. Also, our Online-BLS has low standard deviations, which means with excellent stability for different experimental trials. The average and SD of the online update time are shown in Figure 1. First, our Online-BLS has the shortest online update time, indicating that our method is very efficient. Second, we find that the standard deviation of the online update time of I-BLS increases with the number of instances. These results are also consistent with the time complexity analysis in Section 4.2. Figure 2 shows the convergence curves of all the methods. The sum of the online cumulative error (OCE) and OCA is one. Online-BLS consistently converges rapidly and outperforms all the baselines at almost all time steps on

Method	IS	USPS	Letter	Adult	Shuttle	MNIST
I-BLS	73.6 ± 19.80	61.1 ± 40.10	59.4 ± 27.30	71.3 ± 13.60	86.6 ± 20.10	83.5 ± 24.40
BLS-CIL	83.6 ± 0.423	93.7 ± 0.239	79.7 ± 0.711	75.4 ± 0.020	95.9 ± 0.299	89.9 ± 0.180
RI-BLS	89.9 ± 0.668	92.8 ± 0.228	87.6 ± 0.541	72.0 ± 0.856	90.2 ± 1.100	89.9 ± 0.246
Ours w/o EOUS	90.8 ± 0.229	93.6 ± 0.386	88.9 ± 0.137	76.4 ± 0.050	98.2 ± 0.026	92.5 ± 0.105
Ours	90.8 ± 0.229	93.6 ± 0.386	88.9 ± 0.137	76.4 ± 0.051	98.2 ± 0.026	92.5 ± 0.105

Table 3: Average and SD of OCA (%). Note: Bold indicates the best result, and underlining denotes the second-best result.

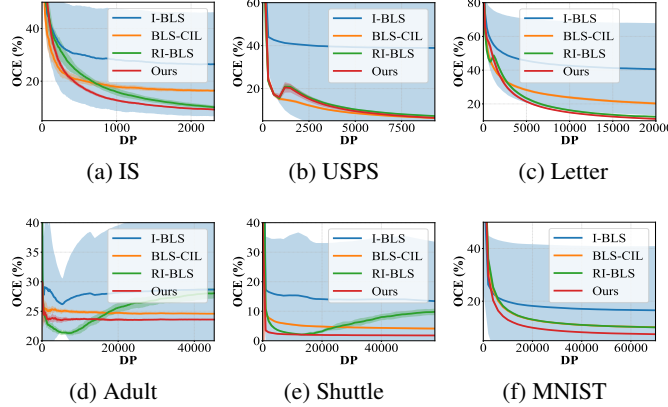


Figure 2: Convergence curves of average and SD. Ours w/o EOUS is omitted because its results are consistent with those of Ours.

all datasets. It also reaffirms the effectiveness of our method.

5.2 Parameter Sensitivity Analysis

Our proposed Online-BLS comes with several tuning parameters, including the enhancement nodes n_3 . The impact of different n_3 on the average OCE is shown in Figure 3. First, our method consistently achieves the lowest average OCE compared to all baselines on all n_3 cases across the six datasets. Second, we find that the average OCE of I-BLS changes significantly with different n_3 . This is because I-BLS is very unstable. That is, the accuracy of I-BLS in some trials is close to that of random guessing cases. Based on the above results, we can safely conclude that Online-BLS is robust to changes of n_3 . Hence, we simply set n_3 to 1,000 on all datasets and did not adjust it for different datasets.

5.3 Ablation Study

Our framework has two main parts, EWEA and EOUS. Amongst them, EWEA is an inseparable part of Online-BLS. Thus, we examine the validity of EOUS in this section. From Table 3 and Figure 1, we can find that EOUS can significantly reduce online update time while maintaining model accuracy. Hence, we can conclude that EOUS is an efficient algorithm that can significantly reduce the online update overhead of Online-BLS.

5.4 Experiments with Concept Drift Dataset

In this section, the effectiveness and flexibility of our Online-BLS are validated in the concept drift scenario. To learn

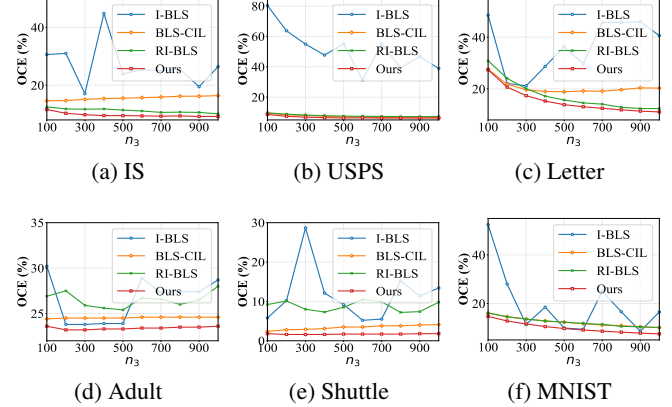


Figure 3: Average OCE under different n_3 values. Ours w/o EOUS is omitted because its results are consistent with those of Ours.

non-stationary data streams, we adopt a forgetting factor to force our Online-BLS to assign larger weights to new arrivals. Specifically, we simply set it to 0.99 for all datasets. We compare our method with two classes of baselines used for data stream classification with concept drift. The first category is online machine learning algorithms, including HT [Hulten *et al.*, 2001] and ARF [Gomes *et al.*, 2017]. The second one is SOTA online deep learning models such as HBP [Sahoo *et al.*, 2018], ADL [Ashfahani and Pratama, 2019], CAND [Gunasekara *et al.*, 2022], ATNN [Wen *et al.*, 2024], and EODL [Su *et al.*, 2024]. Beyond OCA, four metrics are used. They are Balanced Accuracy (BACC), Average Balanced Accuracy (AVRBACC), F1 score (F1), and Matthews Correlation Coefficient (MCC). It is worth noting that all the metrics used in this paper, except OCE, are such that larger values represent better model performance. The details of these metrics can also be found in Appendix C. The parameter settings of our method are consistent with those in section 5.1. Tables 4, 5, 6, and 7 demonstrate the final results on the Hyperplane, SEA, Electricity, and CoverType datasets, respectively.

To make the experimental conclusions more reliable, the results of all baseline methods are directly cited from the corresponding papers and that of Online-BLS with forgetting factor (denoted with Ada.) are averaged over 10 independent experiments. Firstly, ours (Ada.) surpasses typical online machine learning algorithms with a large gap, which benefits from the random feature mapping of BLS that can extract effective broad features. Additionally, ours (Ada.) out-

Method	OCA (\uparrow)	BACC (\uparrow)	AVRBACC (\uparrow)
HT	85.1	86.7	85.4
ARF	76.8	76.2	76.2
HBP	87.0	<u>91.0</u>	86.6
ADL	77.3	80.7	77.2
CAND	88.1	89.8	87.9
EODL	89.5	90.5	89.2
Ours (Ada.)	92.6	92.6	91.7

Table 4: Experimental results (%) on Hyperplane dataset. Note: Bold indicates the best result, and underlining denotes the second-best result.

Method	OCA (\uparrow)	BACC (\uparrow)	AVRBACC (\uparrow)
HT	81.1	82.0	79.4
ARF	<u>83.8</u>	86.5	81.5
HBP	<u>82.1</u>	82.5	78.7
ADL	60.1	49.8	49.9
CAND	79.7	82.8	76.7
EODL	82.5	83.2	79.4
Ours (Ada.)	85.2	<u>83.3</u>	82.6

Table 5: Experimental results (%) on SEA dataset. Note: Bold indicates the best result, and underlining denotes the second-best result.

Method	OCA/MCC	BACC/F1	AVRBACC
HT	77.0/-	74.3/-	74.7
ARF	72.8/-	76.1/-	69.3
HBP	74.8/-	79.6/-	70.3
ADL	74.9/-	81.6/-	70.7
CAND	78.5/-	<u>83.7/-</u>	<u>76.4</u>
ATNN	<u>83.6/66.0</u>	-/83.0	-
EODL	78.0/-	83.5/-	76.2
Ours (Ada.)	86.8/72.9	86.2/86.4	86.9

Table 6: Experimental results (%) on Electricity dataset. Note: Bold indicates the best result, and underlining denotes the second-best result.

Method	OCA/MCC	BACC/F1	AVRBACC
HT	80.1/-	73.0/-	70.4
ARF	83.7/-	80.9/-	64.2
HBP	91.2/-	82.5/-	74.7
ADL	90.5/-	86.7/-	76.8
CAND	92.8/-	85.4/-	79.2
ATNN	<u>92.7/89.0</u>	-/87.0	-
EODL	<u>93.5/-</u>	90.0/-	81.0
Ours (Ada.)	94.3/90.9	89.7/90.0	88.2

Table 7: Experimental results (%) on CoverType dataset. Note: Bold indicates the best result, and underlining denotes the second-best result.

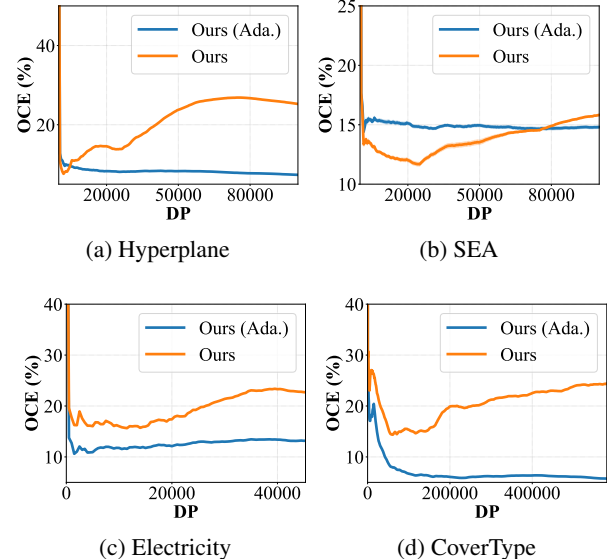


Figure 4: Average and SD of convergence curves of Online-BLS with and without forgetting factor on non-stationary datasets.

performs existing online deep learning methods in almost all metrics. We conjecture that this is due to the fact that the derivation of our method is based on a closed-form solution, which provides a good guarantee of the optimality of the solution updated online. Figure 4 shows the convergence curves of Online-BLS with and without forgetting factors. From Figure 4 we find that the average OCE of Online-BLS increases significantly as concept drift occurs, while ours (Ada.) can maintain a low error rate. Thus, we conclude that by adding a forgetting factor to the historical data, our framework can handle the non-stationary data stream classification task well.

6 Conclusions and Future Works

This paper presented an accurate and efficient Online-BLS framework to solve the suboptimal model weights problem. On the one hand, an EWEA was proposed to improve model accuracy. By replacing the matrix inverse with Cholesky factorization and forward-backward substitution, our proposed Online-BLS becomes accurate. On the other hand, an EOUS was developed and integrated into EWEA to improve the efficiency of our online update method. Through the integration with EWEA and EOUS, Our Online-BLS framework can be accurate and efficient. Theoretical analysis also proves that Online-BLS has excellent error bound and time complexity. In addition, this paper proposed a simple solution for the concept drift problem by adding a forgetting factor to historical data, which also indicates the flexibility and extensibility of our Online-BLS framework. Experiments on stationary and non-stationary datasets demonstrate the superiority and high efficiency of Online-BLS. This work is the first significant attempt to learn BLS models online. In the future, we will consider the issue of class imbalance in online data streams to improve the model performance further.

References

[Ashfahani and Pratama, 2019] Andri Ashfahani and Mardhika Pratama. Autonomous deep learning: Continual learning approach for dynamic environments. In *Proceedings of the 2019 SIAM international conference on data mining*, pages 666–674. SIAM, 2019.

[Bifet *et al.*, 2010] Albert Bifet, Geoff Holmes, and Bernhard Pfahringer. Leveraging bagging for evolving data streams. In *Machine Learning and Knowledge Discovery in Databases: European Conference, ECML PKDD 2010, Barcelona, Spain, September 20–24, 2010, Proceedings, Part I* 21, pages 135–150. Springer, 2010.

[Chen and Liu, 2018] C. L. Philip Chen and Zhulin Liu. Broad learning system: An effective and efficient incremental learning system without the need for deep architecture. *IEEE Transactions on Neural Networks and Learning Systems*, 29(1):10–24, 2018.

[Chen *et al.*, 2019] C. L. Philip Chen, Zhulin Liu, and Shuang Feng. Universal approximation capability of broad learning system and its structural variations. *IEEE Transactions on Neural Networks and Learning Systems*, 30(4):1191–1204, 2019.

[Crammer *et al.*, 2006] Koby Crammer, Ofer Dekel, Joseph Keshet, Shai Shalev-Shwartz, Yoram Singer, and Manfred K Warmuth. Online passive-aggressive algorithms. *Journal of Machine Learning Research*, 7(3), 2006.

[Du *et al.*, 2024] Jie Du, Peng Liu, Chi-Man Vong, Chuangquan Chen, Tianfu Wang, and C. L. Philip Chen. Class-incremental learning method with fast update and high retainability based on broad learning system. *IEEE Transactions on Neural Networks and Learning Systems*, 35(8):11332–11345, 2024.

[Elwell and Polikar, 2011] Ryan Elwell and Robi Polikar. Incremental learning of concept drift in nonstationary environments. *IEEE Transactions on Neural Networks*, 22(10):1517–1531, 2011.

[Fu *et al.*, 2022] Yang Fu, Hongrui Cao, Xuefeng Chen, and Jianming Ding. Task-incremental broad learning system for multi-component intelligent fault diagnosis of machinery. *Knowledge-Based Systems*, 246:108730, 2022.

[Gill *et al.*, 1974] Philip E Gill, Gene H Golub, Walter Murray, and Michael A Saunders. Methods for modifying matrix factorizations. *Mathematics of computation*, 28(126):505–535, 1974.

[Gomes *et al.*, 2017] Heitor M Gomes, Albert Bifet, Jesse Read, Jean Paul Barddal, Fabrício Enembreck, Bernhard Pfahringer, Geoff Holmes, and Talel Abdessalem. Adaptive random forests for evolving data stream classification. *Machine Learning*, 106:1469–1495, 2017.

[Gong *et al.*, 2022] Xinrong Gong, Tong Zhang, C. L. Philip Chen, and Zhulin Liu. Research review for broad learning system: Algorithms, theory, and applications. *IEEE Transactions on Cybernetics*, 52(9):8922–8950, 2022.

[Gong *et al.*, 2024] Xinrong Gong, C. L. Philip Chen, Bin Hu, and Tong Zhang. Ciabl: Completeness-induced adaptive broad learning for cross-subject emotion recognition with eeg and eye movement signals. *IEEE Transactions on Affective Computing*, 15(4):1970–1984, 2024.

[Greville, 1960] TNE Greville. Some applications of the pseudoinverse of a matrix. *SIAM review*, 2(1):15–22, 1960.

[Gunasekara *et al.*, 2022] Nuwan Gunasekara, Heitor Murilo Gomes, Bernhard Pfahringer, and Albert Bifet. Online hyperparameter optimization for streaming neural networks. In *2022 international joint conference on neural networks (IJCNN)*, pages 1–9. IEEE, 2022.

[Gunasekara *et al.*, 2023] Nuwan Gunasekara, Bernhard Pfahringer, Heitor Murilo Gomes, and Albert Bifet. Survey on online streaming continual learning. In *IJCAI*, pages 6628–6637, 2023.

[Guo *et al.*, 2024] Jifeng Guo, Zhulin Liu, and C. L. Philip Chen. An incremental-self-training-guided semi-supervised broad learning system. *IEEE Transactions on Neural Networks and Learning Systems*, pages 1–15, 2024.

[Higham, 2002] Nicholas J Higham. *Accuracy and stability of numerical algorithms*. SIAM, 2002.

[Hoi *et al.*, 2021] Steven CH Hoi, Doyen Sahoo, Jing Lu, and Peilin Zhao. Online learning: A comprehensive survey. *Neurocomputing*, 459:249–289, 2021.

[Hu *et al.*, 2015] Yong Hu, Xiangzhou Zhang, Bin Feng, Kang Xie, and Mei Liu. itrade: A mobile data-driven stock trading system with concept drift adaptation. *International Journal of Data Warehousing and Mining (IJDWM)*, 11(1):66–83, 2015.

[Hulten *et al.*, 2001] Geoff Hulten, Laurie Spencer, and Pedro Domingos. Mining time-changing data streams. In *Proceedings of the Seventh ACM SIGKDD International Conference on Knowledge Discovery and Data Mining, KDD ’01*, page 97–106, New York, NY, USA, 2001. Association for Computing Machinery.

[Larochelle *et al.*, 2009] Hugo Larochelle, Yoshua Bengio, Jérôme Louradour, and Pascal Lamblin. Exploring strategies for training deep neural networks. *Journal of machine learning research*, 10(1), 2009.

[Lei *et al.*, 2024] Chunyu Lei, Jifeng Guo, and C. L. Philip Chen. Convbls: An effective and efficient incremental convolutional broad learning system combining deep and broad representations. *IEEE Transactions on Artificial Intelligence*, 5(10):5075–5089, 2024.

[Rosenblatt, 1958] Frank Rosenblatt. The perceptron: a probabilistic model for information storage and organization in the brain. *Psychological review*, 65(6):386, 1958.

[Sahoo *et al.*, 2018] Doyen Sahoo, Quang Pham, Jing Lu, and Steven CH Hoi. Online deep learning: learning deep neural networks on the fly. In *Proceedings of the 27th*

International Joint Conference on Artificial Intelligence, pages 2660–2666, 2018.

[SEGER, 2007] M SEGER. Low rank update for the cholesky decomposition. *Technical Report*, 2007.

[Su *et al.*, 2024] Rui Su, Husheng Guo, and Wenjian Wang. Elastic online deep learning for dynamic streaming data. *Information Sciences*, page 120799, 2024.

[Swithinbank *et al.*, 1977] Charles Swithinbank, Paul Mc-Clain, and Patricia Little. Drift tracks of antarctic icebergs. *Polar Record*, 18(116):495–501, 1977.

[Wen *et al.*, 2024] YiMin Wen, Xiang Liu, and Hang Yu. Adaptive tree-like neural network: Overcoming catastrophic forgetting to classify streaming data with concept drifts. *Knowledge-Based Systems*, 293:111636, 2024.

[Yuan *et al.*, 2022] Liheng Yuan, Heng Li, Beihao Xia, Cuiying Gao, Mingyue Liu, Wei Yuan, and Xinge You. Recent advances in concept drift adaptation methods for deep learning. In *IJCAI*, pages 5654–5661, 2022.

[Yun *et al.*, 2024] Fan Yun, Zhiwen Yu, Kaixiang Yang, and C. L. Philip Chen. Adaboost-stacking based on incremental broad learning system. *IEEE Transactions on Knowledge and Data Engineering*, 36(12):7585–7599, 2024.

[Zhang *et al.*, 2021] Tong Zhang, Chunyu Lei, Zongyan Zhang, Xian-Bing Meng, and C. L. Philip Chen. Asnas: Adaptive scalable neural architecture search with reinforced evolutionary algorithm for deep learning. *IEEE Transactions on Evolutionary Computation*, 25(5):830–841, 2021.

[Zhang *et al.*, 2024] Zongyan Zhang, Haohan Weng, Tong Zhang, and C. L. Philip Chen. A broad generative network for two-stage image outpainting. *IEEE Transactions on Neural Networks and Learning Systems*, 35(9):12731–12745, 2024.

[Zhong *et al.*, 2024] Linjun Zhong, C. L. Philip Chen, Jifeng Guo, and Tong Zhang. Robust incremental broad learning system for data streams of uncertain scale. *IEEE Transactions on Neural Networks and Learning Systems*, pages 1–14, 2024.

[Zinkevich, 2003] Martin Zinkevich. Online convex programming and generalized infinitesimal gradient ascent. In *Proceedings of the 20th international conference on machine learning (icml-03)*, pages 928–936, 2003.

A Incremental Broad Learning Systems

In this section, we introduce the vanilla BLS and several existing incremental broad learning algorithms that can be used for online learning tasks.

A.1 BLS and I-BLS

BLS [Chen and Liu, 2018] is essentially equivalent to a ridge regression model, except that it utilizes stochastic transformations and nonlinear mapping to extract nonlinear representations. Assume that the first input sample is $\mathbf{x}_1 \in \mathbb{R}^d$, where d is the number of feature dimensions. The i -th feature node group $\mathbf{z}_i \in \mathbb{R}^{n_1}$ is defined as:

$$\mathbf{z}_i^\top = \phi(\mathbf{x}_1^\top \mathbf{W}_{f_i} + \beta_{f_i}^\top), i = 1, 2, \dots, n_2, \quad (21)$$

where $\mathbf{W}_{f_i} \in \mathbb{R}^{d \times n_1}$ and $\beta_{f_i} \in \mathbb{R}^{n_1}$ are randomly generated. $\phi(\cdot)$ represents the selected activation function. Combining all the feature node groups as $\mathbf{z}^\top \triangleq [\mathbf{z}_1^\top, \mathbf{z}_2^\top, \dots, \mathbf{z}_{n_2}^\top]$, the j -th enhancement node group $\mathbf{h}_j \in \mathbb{R}^{n_3}$ can be represented as:

$$\mathbf{h}_j^\top = \sigma(\mathbf{z}^\top \mathbf{W}_{e_j} + \beta_{e_j}^\top), j = 1, 2, \dots, n_4, \quad (22)$$

where $\mathbf{W}_{e_j} \in \mathbb{R}^{n_1 n_2 \times n_3}$ and $\beta_{e_j} \in \mathbb{R}^{n_3}$ are randomly sampled from a given distribution. $\sigma(\cdot)$ denotes a non-linear activation function. Defining broad feature of \mathbf{x}_1 as $\mathbf{a}_1^\top \triangleq [\mathbf{z}^\top | \mathbf{h}_1^\top, \dots, \mathbf{h}_{n_4}^\top]$, the final model weights $\mathbf{W}^{(1)}$ are estimated as: $\mathbf{W}^{(1)} = (\mathbf{a}_1^\top)^+ \mathbf{y}_1^\top$, where \mathbf{y}_1 denotes the target vector of \mathbf{x}_1 and $(\mathbf{a}_1^\top)^+ = (\mathbf{a}_1 \mathbf{a}_1^\top + \lambda \mathbf{I})^{-1} \mathbf{a}_1$. \mathbf{I} is an identity matrix, and λ is used to control the complexity of BLS. When the k -th training sample \mathbf{x}_k arrives, its broad feature $\mathbf{a}_k \in \mathbb{R}^m$ ($m \triangleq n_1 n_2 + n_3 n_4$) is first obtained via substituting \mathbf{x}_k into equations 1 and 2. Then, the updated weight matrix $\mathbf{W}^{(k)}$ is:

$$\mathbf{W}^{(k)} = ([\mathbf{a}_1, \mathbf{a}_2, \dots, \mathbf{a}_k]^\top)^+ [\mathbf{y}_1, \mathbf{y}_2, \dots, \mathbf{y}_k]^\top,$$

where $([\mathbf{a}_1, \mathbf{a}_2, \dots, \mathbf{a}_k]^\top)^+ = [([\mathbf{a}_1, \mathbf{a}_2, \dots, \mathbf{a}_{k-1}]^\top)^+ - \mathbf{F} \mathbf{D}^\top | \mathbf{F}]$, $\mathbf{D}^\top = \mathbf{a}_k^\top ([\mathbf{a}_1, \mathbf{a}_2, \dots, \mathbf{a}_{k-1}]^\top)^+$, $\mathbf{Q} = \mathbf{a}_k^\top - \mathbf{D}^\top [\mathbf{a}_1, \mathbf{a}_2, \dots, \mathbf{a}_{k-1}]^\top$, and

$$\mathbf{F} = \begin{cases} \mathbf{Q}^+ & \text{if } \mathbf{Q} \neq 0 \\ ([\mathbf{a}_1, \mathbf{a}_2, \dots, \mathbf{a}_{k-1}]^\top)^+ \mathbf{D} (1 + \mathbf{D}^\top \mathbf{D})^{-1} & \text{if } \mathbf{Q} = 0. \end{cases}$$

A.2 RI-BLS

To remedy the drawbacks of long training time and poor accuracy of I-BLS, RI-BLS [Zhong *et al.*, 2024] has been proposed, which devises an update strategy for the weight matrix by recursively computing two memory matrices. During the initialization training phase (i.e., RI-BLS receives the first training sample), the estimated weight is

$$\mathbf{W}^{(1)} = (\mathbf{U}^{(1)} + \lambda \mathbf{I})^{-1} \mathbf{V}^{(1)},$$

where $\mathbf{U}^{(1)} = \mathbf{a}_1 \mathbf{a}_1^\top$ and $\mathbf{V}^{(1)} = \mathbf{a}_1 \mathbf{y}_1^\top$.

When the k -th sample arrives, we have

$$\mathbf{W}^{(k)} = (\mathbf{U}^{(k)} + \lambda \mathbf{I})^{-1} \mathbf{V}^{(k)},$$

where $\mathbf{U}^{(k)} = \mathbf{U}^{(k-1)} + \mathbf{a}_k \mathbf{a}_k^\top$ and $\mathbf{V}^{(k)} = \mathbf{V}^{(k-1)} + \mathbf{a}_k \mathbf{y}_k^\top$.

A.3 BLS-CIL

Compared to RI-BLS, BLS-CIL [Du *et al.*, 2024] has been proposed, which has an additional class-correlation loss function and was initially designed to address class-incremental tasks. By adding a single training sample at a time, BLS-CIL can be well adapted to online classification tasks. For the initialization training phase, the weight matrix $\mathbf{W}^{(1)}$ can be expressed as $\mathbf{W}^{(1)} = (\mathbf{K}^{(1)})^{-1} \mathbf{a}_1 \mathbf{y}_1^\top$, where $\mathbf{K}^{(1)} = \mathbf{I} + \mathbf{a}_1 \mathbf{a}_1^\top$. After BLS-CIL receives a new sample \mathbf{x}_k , its weight matrix $\mathbf{W}^{(k)}$ can be formalized as

$$\mathbf{W}^{(k)} = \mathbf{W}^{(k-1)} - (\mathbf{K}^{(k)})^{-1} \mathbf{H} \mathbf{W}^{(k-1)} + (\mathbf{K}^{(k)})^{-1} \mathbf{a}_k \mathbf{y}_k^\top,$$

where $\mathbf{K}^{(k)} = \mathbf{K}^{(k-1)} + \mathbf{H}$, $\mathbf{H} = \mathbf{a}_k \mathbf{a}_k^\top + \lambda (\mathbf{a}_{k-1} \mathbf{a}_{k-1}^\top - \mathbf{a}_k \mathbf{a}_{k-1}^\top + \mathbf{a}_k \mathbf{a}_k^\top - \mathbf{a}_{k-1} \mathbf{a}_k^\top)$, and $\lambda = \begin{cases} -\lambda_1 & \text{if } \mathbf{y}_k \neq \mathbf{y}_{k-1} \\ +\lambda_2 & \text{if } \mathbf{y}_k = \mathbf{y}_{k-1} \end{cases}$, where λ_1 and λ_2 are positive hyper-parameters which are responsible for intra-class compact term and inter-class sparse term losses, respectively.

B Datasets

A total of 10 streaming datasets are used in this paper. Among them, there are 6 stationary datasets and 4 non-stationary datasets with concept drift. In the following, we introduce them in detail.

B.1 Stationary Datasets

Image Segment¹: The Image Segment dataset is an image classification dataset described by 19 high-level numerical attributes. Its samples are randomly sampled from a dataset containing 7 outdoor images. The images are manually segmented and assigned a class label to each pixel. Each instance contains a 3×3 region. It has 2,310 samples containing seven classes *brickface*, *sky*, *foliage*, *cement*, *window*, *path*, and *grass*.

USPS²: The USPS dataset is used for the task of handwritten digit classification. The USPS contains 9,298 samples from 10 classes ranging from 0 to 9. Each sample is a 16×16 grayscale image. To facilitate BLS modeling, we flatten each sample into a one-dimensional vector.

Letter³: The Letter dataset is a capital letter in the English alphabet classification dataset. The Letter dataset contains 20,000 samples. Each sample contains 16 primary numeric attributes (statistical moments and edge counts), which are then scaled to an integer value range of 0 to 15.

Adult⁴: The Adult dataset is used for a binary classification task, which determines whether a person earns more than 50k a year based on 14 attributes. It has both numeric and categorical attributes. We first convert categorical attributes to integers that the model can handle easily. Then, samples with missing values are removed and the training and test sets are merged. Eventually, the Adult dataset has a total of 45,222 samples.

¹<https://archive.ics.uci.edu/dataset/50/image+segmentation>

²<https://datasets.activeloop.ai/docs/ml/datasets/usps-dataset/>

³<https://archive.ics.uci.edu/dataset/59/letter+recognition>

⁴<https://archive.ics.uci.edu/dataset/2/adult>

Shuttle⁵: The Shuttle dataset is a seven-class dataset, including *Rad Flow*, *Fpv Close*, *Fpv Open*, *High*, *Bypass*, *Bpv Close*, and *Bpv Open*. There are 9 numerical attributes. Among them, the first attribute is time. Thus, we remove the first column of attributes and use the remaining 8 attributes to predict one of the seven categories.

MNIST⁶: The MNIST dataset is a handwritten digit recognition benchmark. Each sample is a grayscale image with 28×28 pixels. The training and test sets are merged to yield a dataset containing 70,000 samples uniformly distributed from 0 to 9. To adapt to our model, each sample is flattened into a vector and each attribute is normalized to be between 0 and 1.

B.2 Non-stationary Datasets

For non-stationary datasets, we choose two synthetic datasets and two real datasets. These two synthetic datasets, Hyperplane and SEA, are generated using the River⁷ package. The remaining two real datasets are originated from the real world, often with complex unpredictable concept drift.

Hyperplane: The Hyperplane dataset is an artificial binary classification task. Its task is to divide points in a d -dimensional space into two parts by a $d - 1$ dimensional hyperplane. A sample is labelled positive if it satisfies $\sum_{i=1}^d w_i x_i > w_0$ and negative if the opposite is true. By smoothly changing the parameters of the classification hyperplane, concept drift can be added to the generated data stream. Specifically, following [Su *et al.*, 2024], we generate a data stream containing 20 features. Its noise level and drift magnitude are set to 1% and 0.5%, respectively.

SEA: The SEA dataset is also an artificial binary classification dataset. Each sample contains three features, of which only the first two are relevant. If the sum of the first two features exceeds a certain threshold, then it is a positive example, otherwise it is a negative example. There are 4 thresholds to choose from. Concept drift is introduced by switching thresholds at the 25,000-th, 50,000-th, and 75,000-th data points. Moreover, following [Su *et al.*, 2024], the noise level we introduce in the process of data stream generation is 10%.

Electricity⁸: The Electricity dataset is used as a binary classification task, where the goal is to predict if the electricity price of Australian New South Wales will go up or down. In this market, prices are not fixed and are affected by demand and supply of the market. They are set every five minutes. Each sample originally had 8 attributes. Following [Su *et al.*, 2024], we delete the attributes of date and time located in the first two columns and keep the remaining 6 attributes. This dataset contains 45,312 instances and its concepts fluctuate over time.

CoverType⁹: The CoverType dataset predicts 7 forest cover types from 54 feature value of each instance. The feature types include integer and category types. First, we convert

⁵<https://archive.ics.uci.edu/dataset/148/statlog+shuttle>

⁶<http://yann.lecun.com/exdb/mnist/>

⁷<https://github.com/online-ml/river>

⁸<https://sourceforge.net/projects/moa-datastream/files/Datasets/Classification/elecNormNew.arff.zip/download>

⁹<https://archive.ics.uci.edu/dataset/31/covertype>

the categorical type to an integer for ease of handling. Then, the CoverType dataset has 581,012 instances with unknown concept drift.

C Metrics

In this section, we introduce the six metrics used in this paper.

C.1 Online Cumulative Accuracy

The online cumulative accuracy is used to evaluate the overall performance of online learning models and is defined as

$$OCA = \frac{1}{n} \sum_{k=1}^n \mathbb{I}_{(\hat{y}_k = y_k)},$$

where \mathbb{I} is the indicator function. \hat{y}_k and y_k represent the prediction and ground truth of the k -th instance, respectively.

C.2 Online Cumulative Error

The online cumulative error is used to evaluate the overall error rate during the online learning process and is defined as follows:

$$OCE = \frac{1}{n} \sum_{k=1}^n \mathbb{I}_{(\hat{y}_k \neq y_k)},$$

where \mathbb{I} is the indicator function. \hat{y}_k and y_k represent the prediction and ground truth of the k -th instance, respectively. It should be noted that the sum of the online cumulative accuracy and the online cumulative error at the same time step is 1.

C.3 Balanced Accuracy

The balanced accuracy treats all categories equally and thus is more reliable in data streams with imbalanced classes. It is defined as follows:

$$BACC_k = \left(\sum_{i=1}^c \frac{n_{c_i}^T}{n_{c_i}} \right) / c,$$

where $n_{c_i}^T$ and n_{c_i} denote the number of correctly predicted instances and the total number of instances belonging to the i -th class, respectively. c represents the total number of classes, and k is the current time step.

C.4 Average Balanced Accuracy

The average balanced accuracy is the average of the balanced accuracy at each time step, which can reflect the overall performance of the online learning model throughout the learning process. It has the following definition:

$$AVRBACC = \frac{\sum_{k=1}^n BACC_k}{n},$$

where n is the number of instances received by online learning model.

C.5 F1 Score

Since most of the datasets we use are class-balanced, F1 in this context refers to Macro F1 Score. Its definition is

$$F1 = \frac{1}{c} \sum_{i=1}^c \left(2 \frac{R_i \times P_i}{R_i + P_i} \right),$$

where R_i and P_i denote the recall and precision of class i , respectively.

C.6 Matthews Correlation Coefficient

The matthews correlation coefficient is generally considered a better metric than F1 score and accuracy. Its essence is a correlation coefficient value between -1 and 1 . The coefficient $+1$, 0 , -1 represent a perfect prediction, an average random prediction, and an inverse prediction, respectively. Taking binary classification as an example, its formula is

$$MCC =$$

$$\frac{TP \times TN - FP \times FN}{\sqrt{(TP + FP)(TP + FN)(TN + FP)(TN + FN)}},$$

where TP , TN , FP , and FN denote the number of true positive, the number of true negative, the number of false positive, and the number of false negative, respectively. In fact, we call sklearn's function¹⁰ to acquire the matthews correlation coefficient.

¹⁰https://scikit-learn.org/stable/modules/generated/sklearn.metrics.matthews_corrcoef.html